EPJ Web of Conferences **140**, 09005 (2017) DOI: 10.1051/epjconf/201714009005
Powders & Grains 2017

Structural changes in wet granular matter due to drainage

Prapanch Nair[1,⋆] and *Thorsten* Pöschel[1]

[1] *Institute for Multiscale Simulation, Friedrich-Alexander-Universität Erlangen-Nürnberg, Germany*

Abstract. Unsaturated wet granular media are usually modelled using force laws based on analytical and empirical results of liquid bridge forces between pairs of grains. These models make ad-hoc assumptions on the liquid volume present in the bridges and its distribution. The force between grains and rupture criterion of the bridge are a function of this assumed volume of liquid, in addition to other parameters like contact angle of the liquid, geometry of the grains and the inter grain distance. To study the initial volume and morphology of liquid bridges, hydrodynamic simulation of dynamic effects leading to formation of liquid bridges at grain scale are indispensable. We use a Smoothed Particle Hydrodynamics algorithm to simulate the hydrodynamics of the evolution of the free surface using a novel freesurface-capillary model, inspired by the molecular basis of surface tension. We present validations for the model and simulations of formation and rupture of liquid bridges.

1 Introduction

Unsaturated wet granular media are encountered in a wide range of engineering applications such as in energy sector, pharmaceutics and food industry. Distribution of liquid as bridges between pairs of grains and in more complex shapes between more than two particles leads to complex constitutive behaviour of the material [1]. The formation of liquid bridges between wet particle also cause grain agglomeration which is either desirable (e.g. wet granulation) or undesirable (wet fluidized beds). A better understanding of the 'formation' of liquid bridges will aid in controlling these processes and in arriving at better input parameters for macroscopic simulations. Studies on liquid bridges in literature usually focus on static bridges, and deformation of bridges during stretching and rupture, quasi-statically [2, 3]. Few experimental and theoretical studies have focused on the initial bridge formation process [4], the dynamics due to liquid transfer from grain to the bridge and the hydrodynamics of the rupture of the bridge [5].

Most research that describes dynamics of liquid bridges do so without considering hydrodynamics owing to the difficulty in resolving such effects at low capillary numbers. Empirical models that resulted from experimental studies were summarized by Herminghaus [6], which are used in a number of industrial scale studies as force laws. Capillary bridge force between grains of different sizes (polydisperse) was studied by Cherblanc et. al. [3], where an analytical rupture criterion for liquid bridges was also proposed. A recent Computational Fluid Dynamics simulation by [5] report the underprediction by analytical models, of the rupture criteria for liquid bridges formed by collision of two wet spheres. Another CFD study [7] presents the physics of formation of liquid bridges for given flow conditions. To our knowledge no theoretical study exists that considers the formation of liquid bridges following drainage. In particular, the volume of liquid 'trapped' after the liquid drains through a pair of particles has not been studied. Current advances in meshless methods for fluid dynamics allow simulations of such scenario, overcoming conventional difficulties in CFD related to large density ratio (between liquid and surrounding gas) and coupling with rigid bodies.

Smoothed Particle Hydrodynamics [8] is extensively used in simulation of complex fluid flow involving interactions with rigid bodies and effects of surface tension. A recent free surface model in SPH [9] allows for accurate simulation of flows involving free surfaces and superimposition of surface tension forces on the particle domain. We present and validate this SPH model in three dimensions. The method is then applied to simulate example cases of rupture of liquid bridge between two solids and the formation of liquid bridge between two grains following liquid draining. Visualizations of dynamic evolution of liquid bridges are presented.

2 Formulation

We outline the governing equations that are being solved, and the numerical method namely Incompressible Smoothed Particle Hydrodynamics (ISPH) with the capillary model, here.

⋆e-mail: prapanch.nair@fau.de

2.1 Governing equations

Incompressible isothermal fluid flow is governed by the momentum conservation equations:

$$\frac{D\mathbf{u}}{Dt} = \frac{1}{\rho}\left(-\nabla p + \nabla \cdot (2\mu \mathbf{D}) + \mathbf{f}^B\right), \quad (1)$$

where $\mathbf{u}$ is the velocity, p is the pressure, ρ and μ are the density and coefficient of viscosity of the fluid, respectively, $\mathbf{D} = (\nabla\mathbf{u} + \nabla\mathbf{u}^T)/2$ is the deformation rate tensor, $\mathbf{f}^B$ is the body force per unit mass on the fluid element and t is the time. The momentum equation (eq. 1) is the Navier-Stokes equations written in Lagrangian formulation and D/Dt denotes the material derivative. The mass conservation is ensured through the constraint of divergence free velocity field, $\nabla \cdot \mathbf{u} = 0$. In the incompressible version of SPH (as opposed to the Weakly Compressible version [10],) incompressibility is achieved by solving for a pressure field whose gradient ensures a divergence free velocity field.

2.2 SPH approximation

The basics of SPH algorithm and its fundamentals are widely established and are described in a number of publications [8]. For the purpose of brevity, we here present the SPH descritization of the governing equations, together with terms that account for capillary effects directly. The momentum conservation equation in the SPH formulation reads as:

$$\left(\frac{D\mathbf{u}}{Dt}\right)_a = -\sum_b m_b \left(\frac{p_a}{\rho_a^2} + \frac{p_b}{\rho_b^2}\right)\nabla_a W_{ab} + \sum_b m_b \left(\frac{2\mu}{(\rho_a\rho_b)}\frac{\mathbf{r}_{ab}\cdot\nabla W_{ab}}{r_{ab}^2 + \eta^2}\right)\mathbf{u}_{ab} + \mathbf{F}_a^{\text{int}} + \mathbf{F}^b. \quad (2)$$

Here, the first term on the right hand side represents the acceleration due to pressure gradient and the second term represents the viscous dissipation. The equation is written for the conservation of moment for a discretized fluid particle a, and particles in the neighborhood represented by subscript b. The variables p, ρ and μ represent the pressure, density and viscosity of the fluid, respectively. For incompressible flows, the value of ρ remains the same throughout the fluid. The third term on the RHS represents the acceleration due to pairwise-interparticle force superimposed on the discretized particles and is responsible for the effect of surface tension and contact angle dynamics, and will be described in the next subsection. The fourth term on the RHS represents the body force (gravity) acting on the domain.

2.3 Pairwise forces and capillarity

Following the molecular theory of capillarity [11], Tartakovsky and Meakin [12] proposed a surface tension model and methods for applying macroscopic surface tension coefficient to a Weakly Compressible SPH algorithm

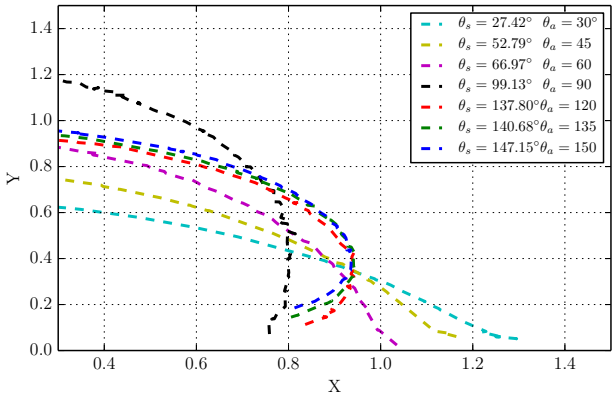

Figure 1: The profile of droplet placed on solid substrate, for different contact angles. θ_s is the contact angle measured by linear regression of six surface particles near the substrate and θ_a is the contact angle given by pairwise force ratio.

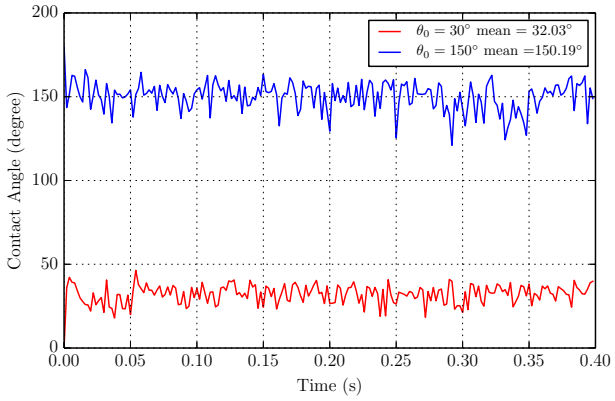

Figure 2: Time variation of the contact angle for the case of $\theta = 30°$ and $\theta = 60°$. The droplets were initiated from the geometry of hemisphere resting on a solid surface.

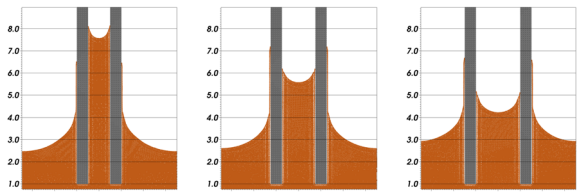

Figure 3: Capillary rise for different diameters (2D)

with an equation of state based on ideal gas law. In addition to mimicking the effect of surface tension, the superimposition of pairwise forces introduces a 'virial' pressure to the fluid, and this additional pressure can be computed for a given particle system. In the case of incompressible fluids with a free surface (single phase), the virial pressure can be treated as an additive term. Though this needs

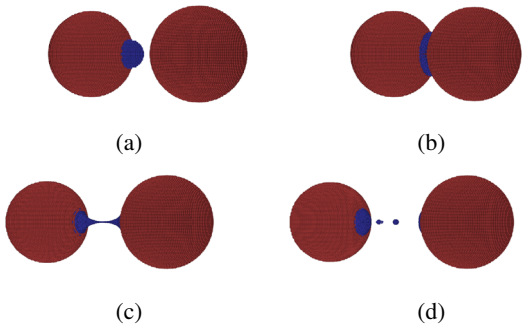

Figure 4: Instances of collision of two rigid spheres with a wet spot on one.

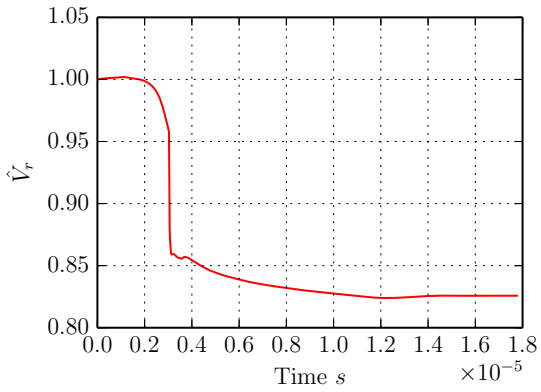

Figure 5: Normalized absolute relative velocity ($\hat{V}_r$) of the colliding grains. The asymptotic value corresponds to the coefficient of restitution

to be corrected for to account for accurate Laplace pressure jump across interfaces, the dynamics of capillary flow would depend only on relative values of pressure, that is, the pressure gradient.

We use the cosine function as given in [12] for the pairwise force and maintain the same cutoff length as the smoothing kernel used for computation of other forces from the continuum model. The pairwise force is given as:

$$\mathbf{F}^{\text{int}}_{ab,\alpha\beta}(r_{ab}) = \begin{cases} -s_{\alpha\beta}\cos\left(\frac{3\pi}{2h}r_{ab}\right) & r_{ab} \le h \times r_{\text{cutoff}} \\ 0 & r_{ab} > h \times r_{\text{cutoff}} \end{cases}. \quad (3)$$

Using this potential and using the Hardy's [11] formula for integrating stresses at a point in a Lagrangian particle model, the partial surface energy due to pairwise interaction force is given by:

$$\mathbf{T}^{\text{int}} = \frac{1}{8}\pi n_\alpha^2 \int_0^\infty \mathbf{F}^{\text{int}}_{\alpha\alpha}(z)dz. \quad (4)$$

For the 5$^{\text{th}}$ order Wendland kernel function [13] used in the current work, this leads to the calibration equation for the surface tension coefficient:

$$\sigma = \frac{0.0134825\pi}{\Delta x} s_{ll} h^5_{\text{ratio}}. \quad (5)$$

Here, h_{ratio} is the ratio of the total cutoff length of the kernel to the initial particle spacing Δx. The strength of the pairwise force is given by s_{ll}. Using different values for strengths of pairwise force, and correspondingly for different ratios for surface energies, different contact angles can be obtained. For the free surface simulations presented here, the contact angle is given by:

$$\cos\theta_0 = \frac{-s_{\alpha\alpha} + 2s_{\alpha\beta}}{s_{\alpha\alpha}}, \quad (6)$$

where θ_0 is the contact angle, $s_{\alpha\alpha}$ is the strength of pairwise potential between liquid and $s_{\alpha\beta}$ is the strength of pairwise potential between particles of different phases, for example, liquid and solid. We integrate the SPH equations using the velocity Verlet integration algorithm [12]

3 Validation and results

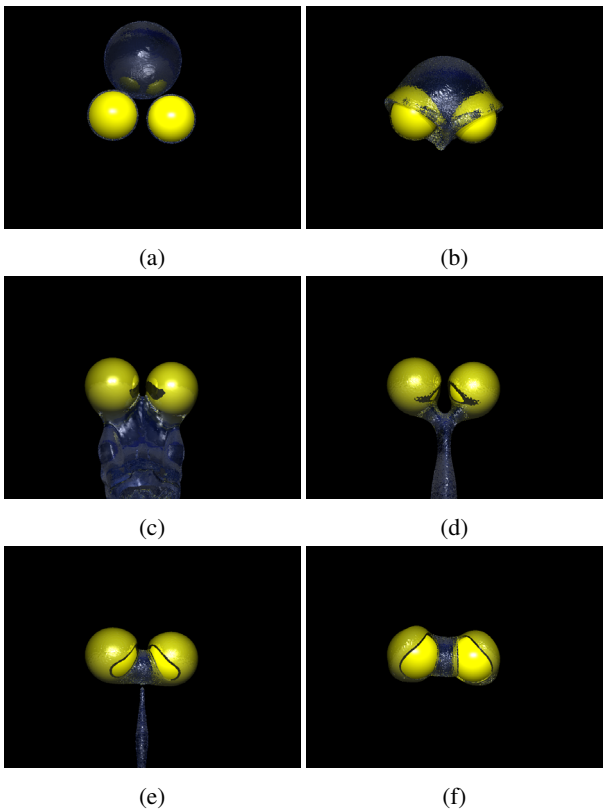

Figure 6: Instance of formation of a liquid bridge following draining of a large liquid drop through a pair of spherical grains

Validation of the surface tension model by an oscillating bubble experiment was performed and will be part of a different detailed publication. Validations of more complex phenomena relevant to the present work, are presented here.

3.1 Contact angle

Equation 6 as a model for wetting phenomena is validated for different contact angles ranging from 30° to 150°. A hemispherical drop is placed on a horizontal solid substrate and is allowed to relax. Figure 1 shows the outer profile of the droplet after a finite time for different contact angles. The time variation of the contact angle after the droplet is allowed to relax from its initial hemispherical position for two extreme contact angles is shown in Fig. 2. The contact angles are measured by linear regression of position of first six surface particles from the substrate.

3.2 Capillary rise in 2D

Table 1: The capillary rise height for different capillary tube diameters (2D)

	Height	
Width (mm)	Analytical	SPH
0.50	5.01	5.12
0.75	2.78	2.95
1.00	1.56	1.31

We perform a numerical experiment with capillary tubes of different diameters immersed in a periodic domain of liquid. The capillary rise height can be analytically derived using balance of pressure due to liquid column and the Laplace pressure jump across curved interfaces. Table 1 shows the comparison of measured capillary rise and the analytical result for different diameters of the capillary tube. The simulations results for different capillary widths are shown in Fig. 3.

3.3 Rupture of capillary bridge

In wet granulation processes, predicting agglomeration of granules is a critical step for successful simulations [14]. In many macro-scale simulations, analytical criteria is used to decide whether capillary bridges formed during collision of two wet particles would sustain for the given approach momenta of the grains. In a recent computational fluid mechanics study [5], it was shown that the analytical cohesion criteria grossly underpredicts the rupture criteria. We perform a similar simulation using the proposed SPH algorithm to corroborate this observation opening up the possibility for deriving accurate agglomeration criteria for complex scenarios involving polydisperse grains and out-of-axis collisions.

Two particles of diameter 50 μm are considered, with a fluid drop of $\approx$ 1072 μm^3 volume on one of the particles. The viscosity and surface tension coefficient of the liquid are 0.001 Nsm^{-2} and 0.071 N/m respectively. The dry particle is imparted a velocity of $5m/s$ towards the wet particle. The moment of rupture is clearly seen in 4, with the formation of two satellite droplets. The coefficient of restitution for the impact can be observed from Fig. 5, as the asymptotic value of normalized relative velocity of the colliding particles. In this case, the restitution coefficient is $e \approx 0.825$.

3.4 Formation of capillary bridge following drainage

The simulation of capillary bridge surfaces in literature usually employ surface energy minimization algorithms [2]. However, the initial liquid volume in the bridge which involves draining of liquid is not given enough attention in literature. We perform simulation of a large liquid droplet impact a pair of grains, and drain through them, resulting in a liquid bridge. Figure 6 shows the different stages of this liquid flow through grains. In Fig. 6b, the liquid drop penetrates the space between grains. In Fig. 6d, a 'Y' shaped configuration of the liquid between the grains pulled down by inertia of liquid is seen. Following this, as see in in Fig. 6e, the bridge begins to be formed when the forked fluid structure straightens and moves upwards due to hydrophilicity of the grain surface. The vertical stem undergoes a rupture at this instant. In Fig. 6f, we see the liquid bridge completely detached and retain a finite fluid volume in it.

4 Conclusion

Using a novel free surface-surface tension model the structural changes of the liquid before formation of liquid bridge following draining of liquid and during its rupture following violent collisions are simulated for example scenarios. These simulations provide confidence for more detailed parametric studies that would result in better force laws, and models to describe liquid bridge formation and rupture.

References

[1] S. Strauch, S. Herminghaus, Soft Matter **8**, 8271 (2012)
[2] C. Semprebon, M. Scheel, S. Herminghaus, R. Seemann, M. Brinkmann, Phys. Rev. E **94**, 012907 (2016)
[3] F. Cherblanc, M.S.E. Youssoufi, C. Saix, F. Soulie, pp. 213–228 (2006)
[4] M. Wu, S. Radl, J.G. Khinast, AIChE Journal **62**, 1877 (2016)
[5] H. Kan, H. Nakamura, S. Watano, Chem Eng Sci **138**, 607 (2015)
[6] S. Herminghaus, Adv Phys **54**, 221 (2005)
[7] Z. Wei, Y. Sun, W. Ding, Z. Wang, Sci China Phys Mech Astron **59**, 694611 (2016)
[8] J.J. Monaghan, Rep Prog Phys **68**, 1703 (2005)
[9] P. Nair, G. Tomar, Comput Fluids **102**, 304 (2014)
[10] E.S. Lee, C. Moulinec, R. Xu, D. Violeau, D. Laurence, P. Stansby, J Comp Phys **227**, 8417 (2008)
[11] J.S. Rowlinson, B. Widom, *Molecular theory of capillarity* (Courier Corporation, 2013)
[12] A.M. Tartakovsky, A. Panchenko, J Comp Phys **305**, 1119 (2016)
[13] K. Szewc, J. Pozorski, J.P. Minier, Int J Numer Meth Eng **92**, 343 (2012)
[14] M. Hussain, J. Kumar, M. Peglow, E. Tsotsas, Chem Eng Sci **101**, 35 (2013)